

Supplemental Data

Lrp5 Controls Bone Formation by Inhibiting Serotonin Synthesis in the Duodenum

Vijay K. Yadav, Je-Hwang Ryu, Nina Suda, Kenji F. Tanaka, Jay A. Gingrich, Günther Schütz, Francis H. Glorieux, Cherie Y. Chiang, Jeffrey D. Zajac, Karl L. Insogna, J. John Mann, Rene Hen, Patricia Ducy, and Gerard Karsenty

Figure S1. Increase in duodenum-derived serotonin in *Lrp5*^{-/-} mice.

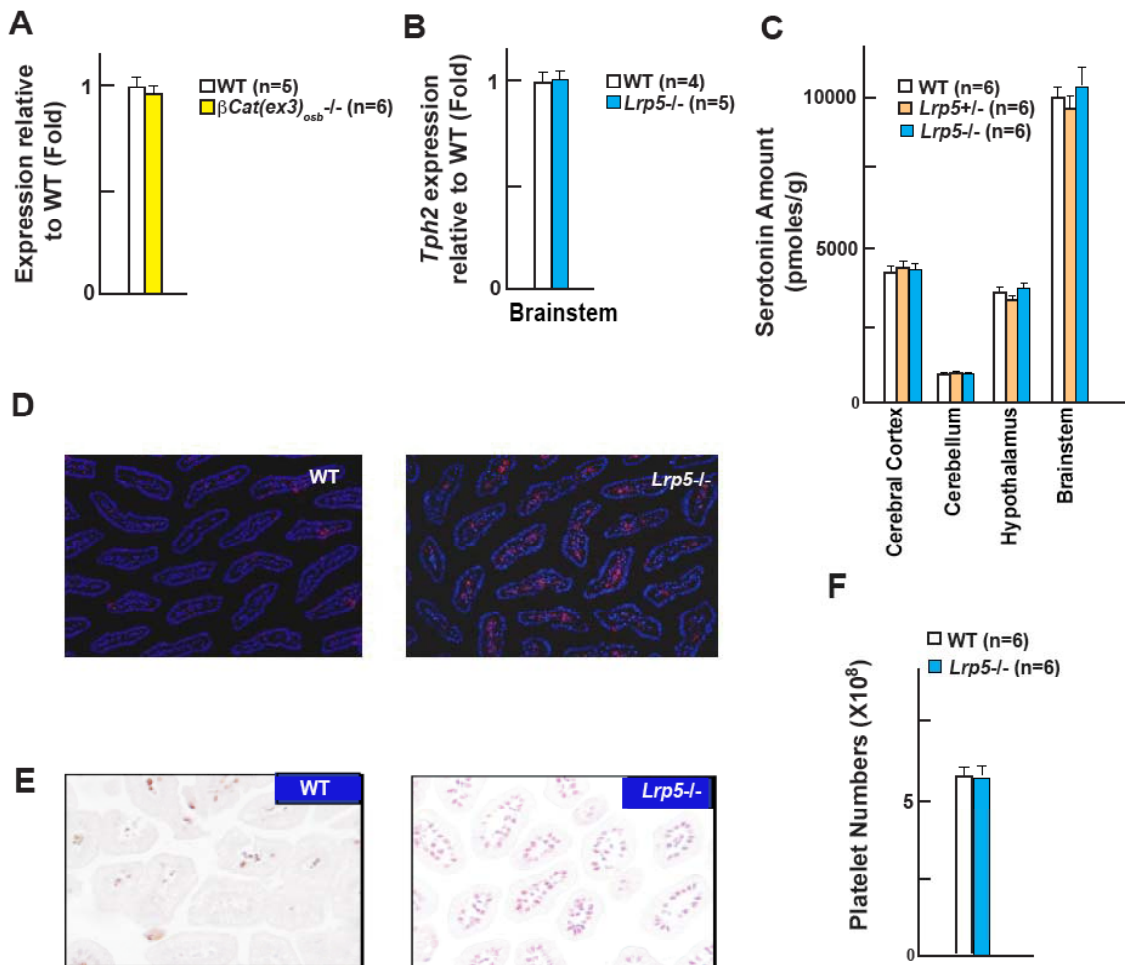


Figure S1.

(A) *Tph1* expression in long bones of WT and β -Catenin(ex3)_{osb}^{-/-} mice.

(B) *Tph2* expression in the brainstem of WT and *Lrp5*^{-/-} mice.

(C) HPLC analysis of serotonin content in different regions of brain in WT, *Lrp5*^{+/-} and *Lrp5*^{-/-} mice.

(D) *In situ* hybridization analysis of *Tph1* expression in the duodenum of WT and *Lrp5*^{-/-} at 1 month of age.

(E) Serotonin immuno-histochemistry in the duodenum of WT and *Lrp5*^{-/-} at 1 month of age.

(F) Platelet numbers in WT and *Lrp5*^{-/-} at 3 months of age.

Figure S1G. Clinical Information for the OPPG patients studied.

Sex/Age	LRP5 Mutation	Bone Mass	Vision	Diagnosis
Male/23 Yrs	1282C>T Arg428>STOP Homozygous	Patient sustained 11 fractures, mostly clavicles and humeri. At referral, low BMD and 9 vertebral compression fractures were noted.	Blind from birth.	OPPG
Female/13 Yrs	1282C>T Arg428>STOP Homozygous	During the first year of life, patient sustained 6 femoral fractures. Treatment with pamidronate was started at 15 months and maintained for 5 years during which BMD increased rapidly and only 3 fractures occurred. The patient remains ambulatory with normal growth and minor deformity of one humerus.	Physical examination at birth revealed only bilateral microphthalmia, and blindness. MRI examination elicited the persistence of the vitreous body.	OPPG
Male/11Yrs	4081C>G Cys1361>Gly Homozygous	Generalized reduction in bone density on thoracolumbar X-ray, Osteopenic DEXA: Neck Of Femur Z score -1.2 (lowest quartile of age matched controls), Lumbar Spine Z score -2.2 (lowest decile of age matched controls). Height for age 10th centile. No specific treatment for bone as yet.	Noted visual problem at 8 weeks. FEVR (Familial exudative vitreoretinopathy) diagnosed, left eye underwent surgery, legally blind, right eye 1/24 vision.	OPPG

Figure S2. Changes in osteoblastic marker genes upon serotonin treatment and brain serotonin levels following diet or pCPA treatment.

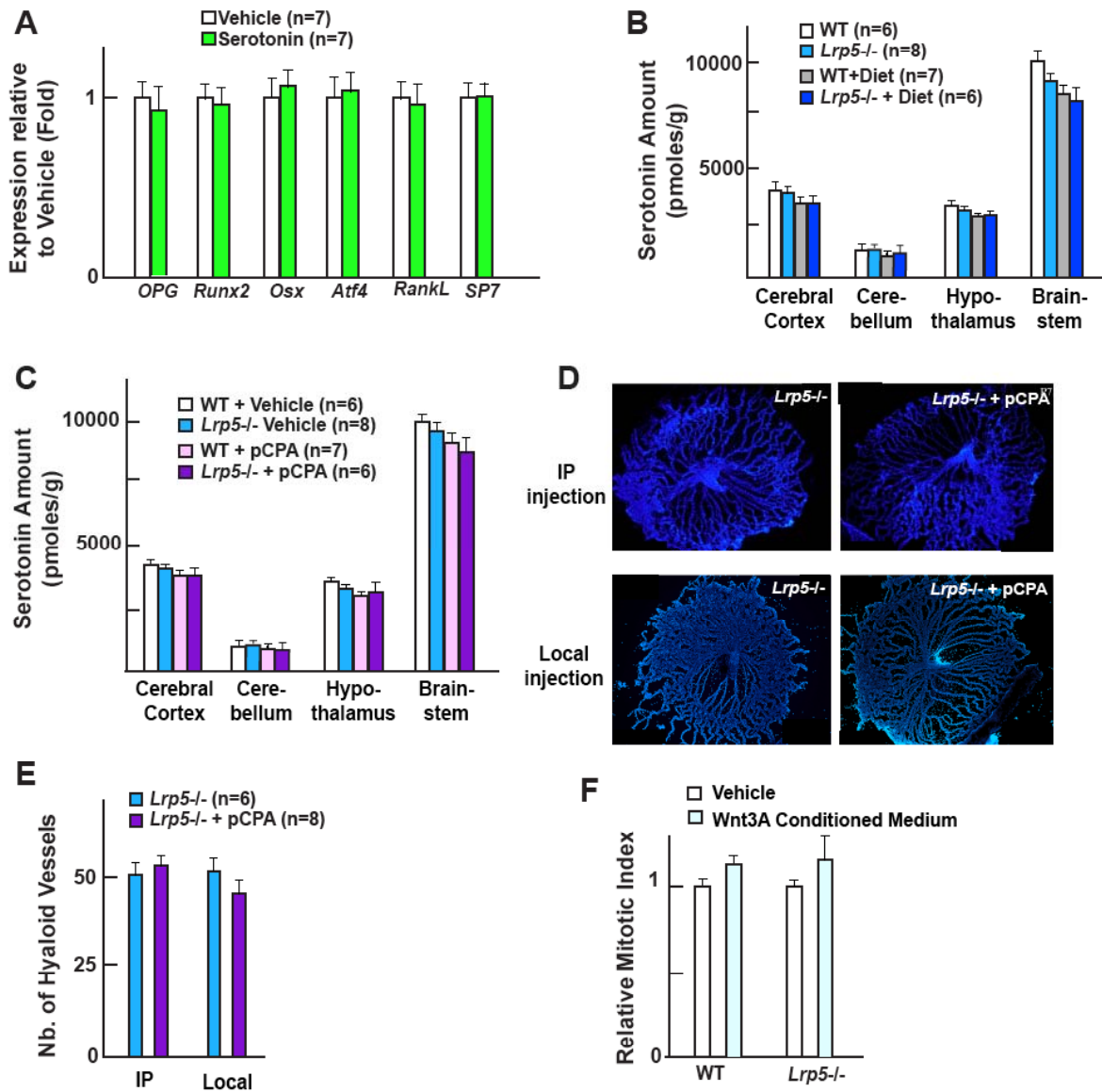


Figure S2

(A) *OPG*, *Runx2*, *Osx*, *Atf4*, *RankL* and *SP7* expression in primary osteoblasts following serotonin (50 μ M) treatment.

(B-C) HPLC analysis of serotonin content in different regions of brain in WT and *Lrp5*^{-/-} mice fed normal or 75% tryptophan-less diet (B) and treated with pCPA (C).

(D-E) Analysis of hyaloid vessels in eyes of *Lrp5*^{-/-} mice that received either vehicle or pCPA through intra-peritoneal or local injection in the eye.

(F) *Ex vivo* proliferation rates of WT and *Lrp5*^{-/-} osteoblasts cultured in the presence of Wnt3A conditioned medium for 24 hours.

Figure S3. Generation of *Lrp5* floxed and floxed knock in mice

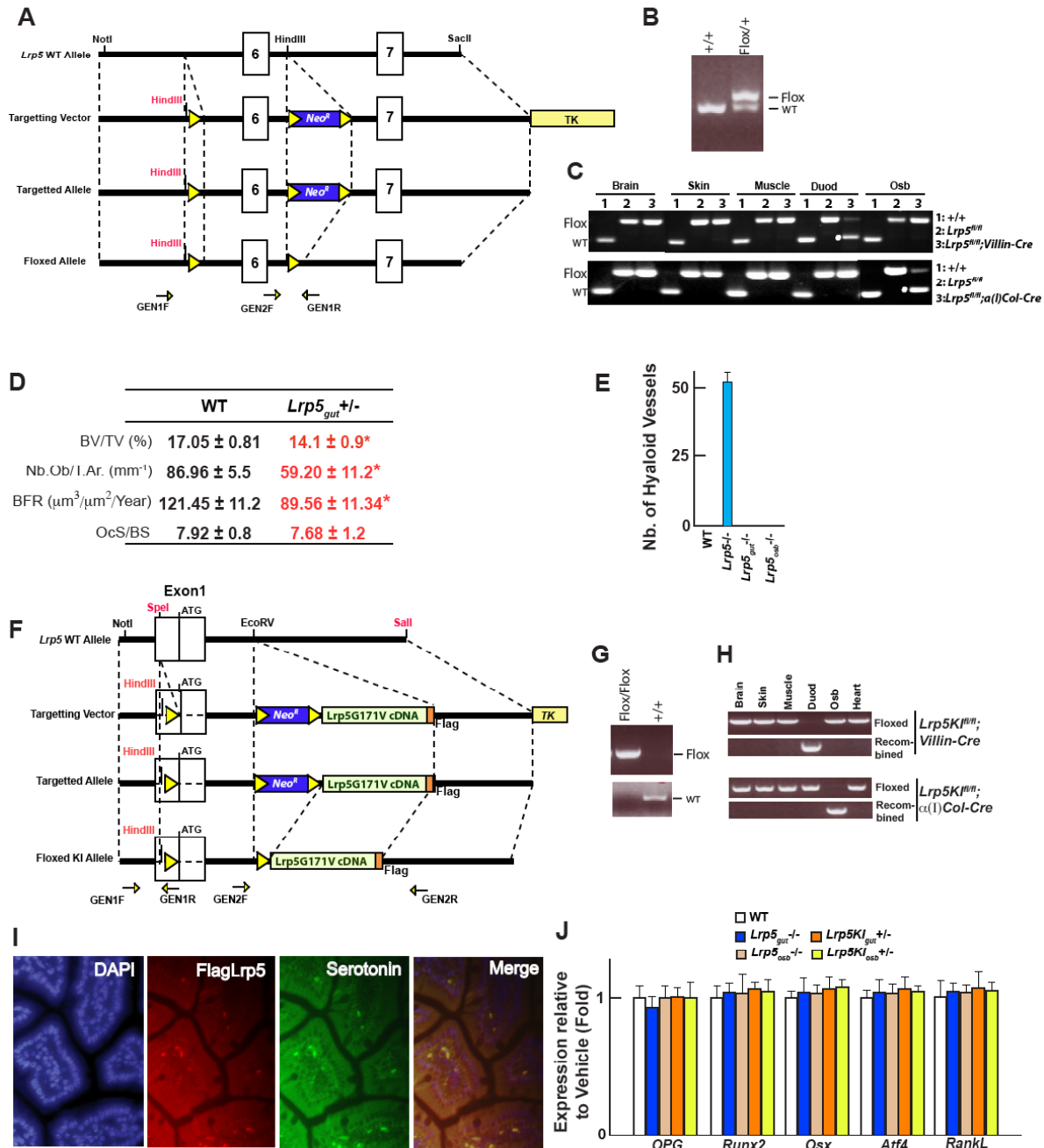


Figure S3

(A-C) Targeting strategy for generating *Lrp5* floxed allele through homologous recombination in embryonic stem (ES) cells (A). PCR genotyping of WT and *Lrp5^{fl/+}* mice (B). Recombination analysis at the *Lrp5* locus in the different tissues of *Lrp5* floxed mice. Asterisks indicate the recombined allele (C).

(D) Histomorphometric analysis of vertebrae of 3 month-old WT and *Lrp5_{gut}^{+/-}* mice.

(E) Analysis of hyaloid vessels in eyes of WT, *Lrp5^{-/-}*, *Lrp5_{gut}^{-/-}* and *Lrp5_{osb}^{-/-}* mice.

(F-H) Targeting strategy for generating *Lrp5* conditional knock in mice through homologous recombination in ES cells (F). PCR genotyping of WT and *Lrp5*^{fl/fl} mice (G). Recombination analysis at the *Lrp5* locus in different tissues of *Lrp5* conditional knock in mice in the gut or osteoblasts (H).

(I) Immuno-histochemical colocalization of serotonin and Flag-Lrp5G171V in the gut of *Lrp5*^{KI_{gut}+/-} mice.

(J) *OPG*, *Runx2*, *Osx*, *Atf4* and *RankL* expression in long bones of WT, *Lrp5*^{gut-/-}, *Lrp5*^{osb-/-}, *Lrp5*^{KI_{gut}+/-} and *Lrp5*^{KI_{osb}+/-} mice.

Figure S4. Generation of *Tph1* floxed mice

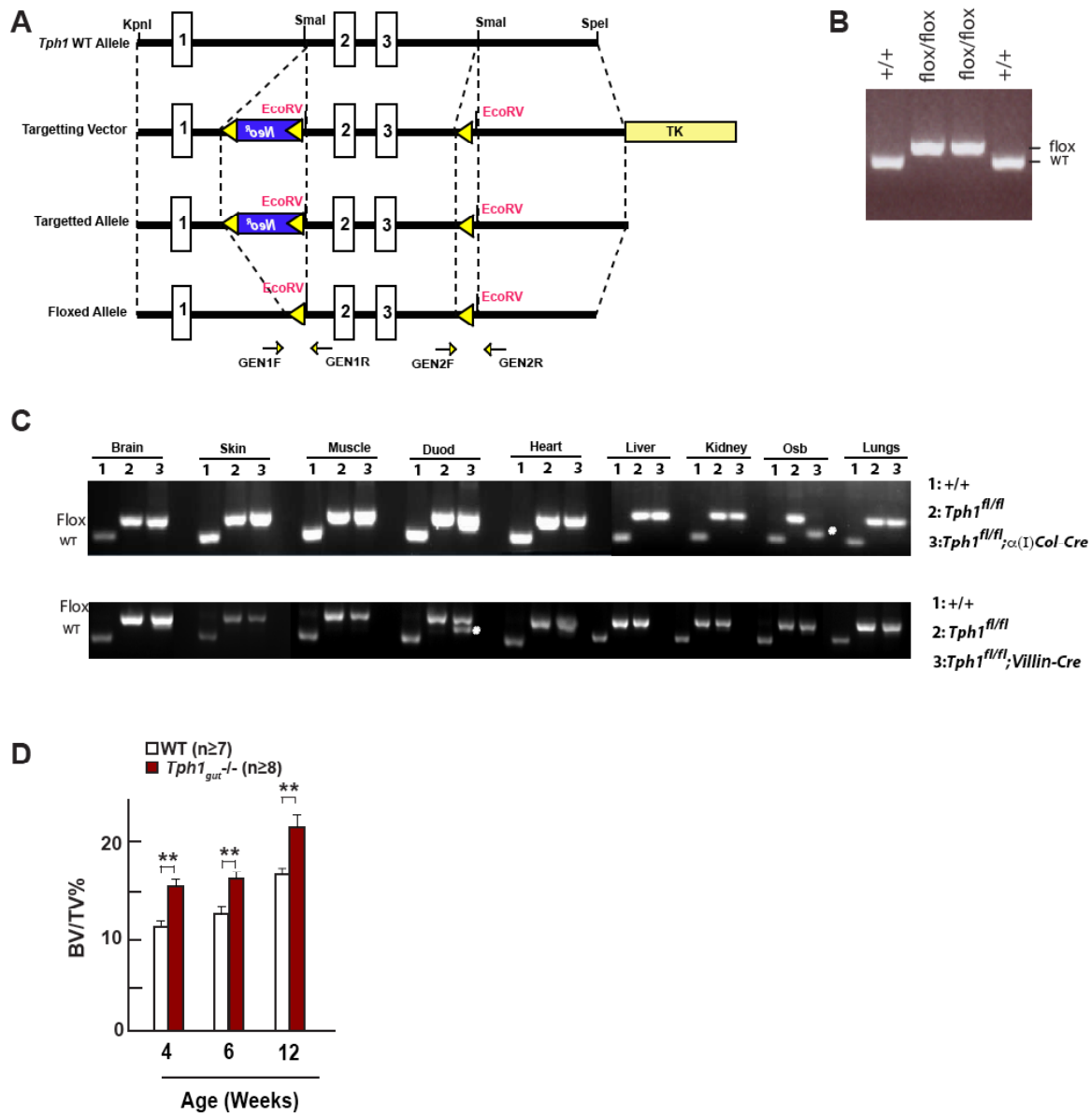


Figure S4

(A-C) Targeting strategy for generating *Tph1* floxed allele through homologous recombination in ES cells (A). PCR genotyping of WT and *Tph1^{fl/fl}* mice (B). Recombination analysis at the *Tph1* locus in different tissues of *Tph1* floxed mice in the gut or osteoblasts. Asterisks indicate the recombined allele (C).

(D) BV/TV% in the WT and *Tph1_{gut}^{-/-}* mice at different ages after birth determined by bone histomorphometry.

Figure S5. Generation and analysis of serotonin receptor-deficient mice

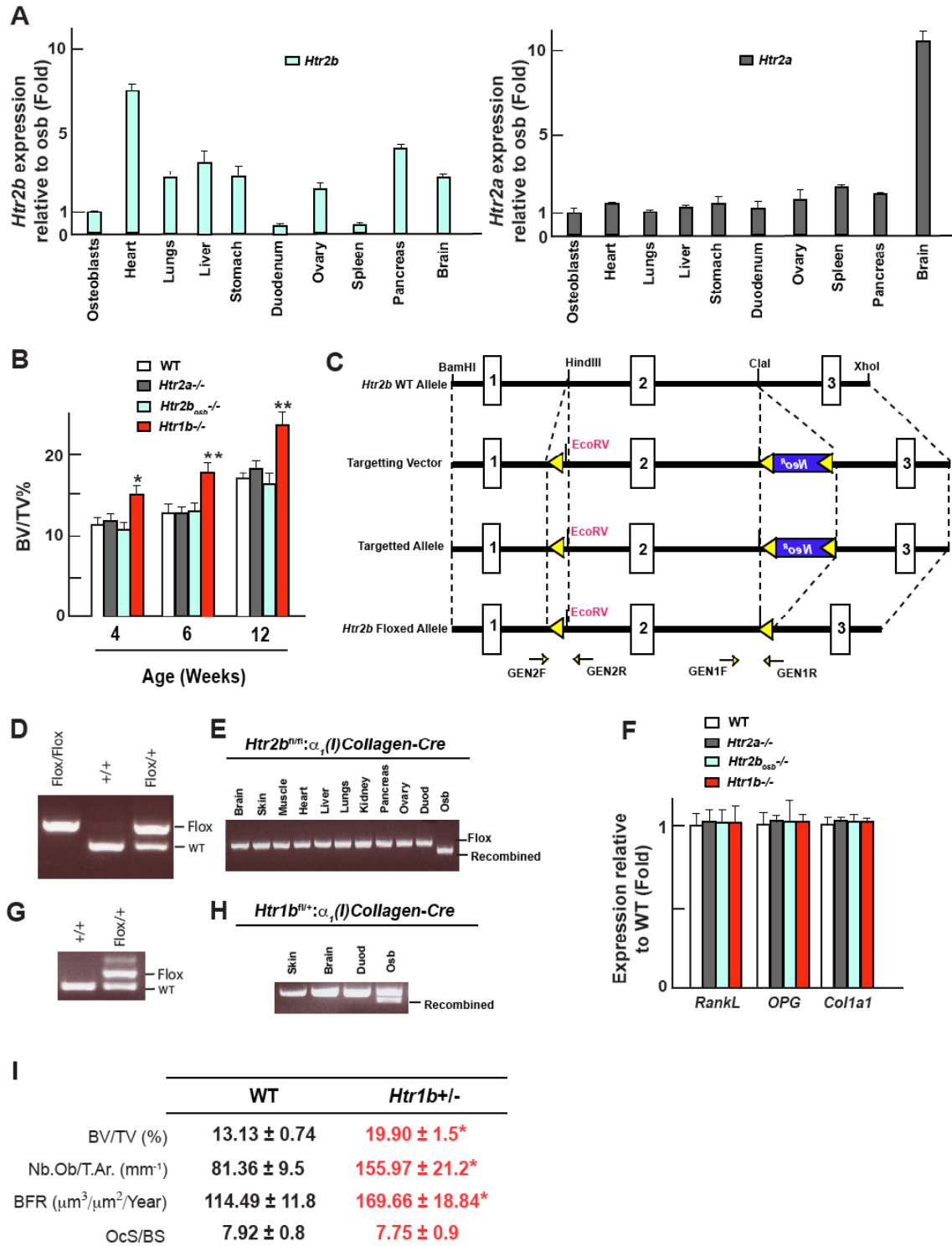


Figure S5

(A) Real-time PCR analysis of *Htr2b* and *Htr2a* expression in different tissues of WT mice (n=3).

(B) BV/TV% in the WT, *Htr2a*^{-/-}, *Htr2b*_{osb}^{-/-} and *Htr1b*^{-/-} mice at different ages after birth determined by bone histomorphometry.

(C-E) Targeting strategy for generating *Htr2b* floxed allele through homologous recombination in ES cells (C). PCR genotyping of WT and *Htr2b*^{fl/fl} mice (D). Recombination analysis at the *Htr2b* locus in the osteoblasts of *Htr2b* floxed mice. Asterisks indicate the recombined allele (E).

(F) *RankL* and *OPG* expression in the long bones of WT, *Htr2a*^{-/-}, *Htr2b*_{osb}^{-/-} and *Htr1b*^{-/-} mice.

(G-H) PCR genotyping of WT and *Htr1b*^{fl/fl} mice (G). Recombination analysis at the *Htr1b* locus in the osteoblasts of *Htr1b* floxed mice. Asterisks indicate the recombined allele (H).

(I) Histomorphometric analysis of vertebrae of 6 week-old WT and *Htr1b*^{+/-} mice.

Figure S6. Identification of the transcription factor downstream of Lrp5 and serotonin


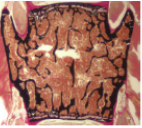

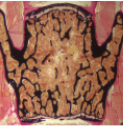
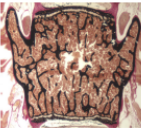
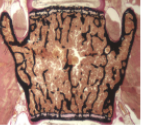



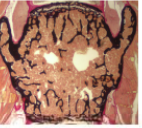
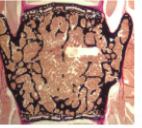
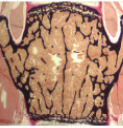
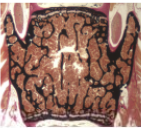
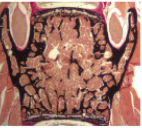

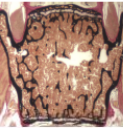
	WT	<i>Lrp5</i> +/-	<i>Runx2</i> +/-	<i>Lrp5</i> +/-; <i>Runx2</i> +/-
				
BV/TV (%)	15.6 ± 0.32	13.8 ± 0.3*	15.8 ± 0.35	12.9 ± 0.32
Nb.Ob/T.Ar. (mm ⁻¹)	76.6 ± 9.2	56.8 ± 7.1	66.2 ± 6.1	54.7 ± 3.1
BFR (μm ³ /μm ² /Year)	104.3 ± 12.1	67.0 ± 8.9	97.3 ± 10.9	65.0 ± 7.9
OcS/BS	7.76 ± 0.4	7.92 ± 0.3	7.75 ± 0.4	7.68 ± 0.9
	WT	<i>Lrp5</i> +/-	<i>Osx</i> +/-	<i>Lrp5</i> +/-; <i>Osx</i> +/-
				
BV/TV (%)	16.1 ± 0.33	13.5 ± 0.2*	16.1 ± 0.28	13.5 ± 0.4
Nb.Ob/T.Ar. (mm ⁻¹)	81.9 ± 9.8	60.7 ± 7.5	66.2 ± 21.1	56.7 ± 7.1
BFR (μm ³ /μm ² /Year)	111.6 ± 12.9	71.6 ± 9.5	105.3 ± 10.9	75.0 ± 7.9
OcS/BS	8.30 ± 0.4	8.47 ± 0.3	7.59 ± 0.8	7.59 ± 0.5
	WT	<i>Lrp5</i> +/-	<i>Atf4</i> +/-	<i>Lrp5</i> +/-; <i>Atf4</i> +/-
				
BV/TV (%)	16.5 ± 0.34	13.1 ± 0.2*	15.2 ± 0.77	12.9 ± 0.95
Nb.Ob/T.Ar. (mm ⁻¹)	71.2 ± 8.5	52.8 ± 6.6	57.6 ± 6.1	53.7 ± 10.1
BFR (μm ³ /μm ² /Year)	96.9 ± 12.0	62.3 ± 8.2	59.2 ± 7.9	75.5 ± 16.5
OcS/BS	7.21 ± 0.3	7.36 ± 0.2	7.85 ± 0.9	7.57 ± 0.4
	WT	<i>Lrp5</i> +/-	<i>Creb_{osb}</i> +/-	<i>Lrp5</i> +/-; <i>Creb_{osb}</i> +/-
				
BV/TV (%)	16.0 ± 0.33	13.4 ± 0.1*	15.5 ± 1.22	9.8 ± 0.36*
Nb.Ob/T.Ar. (mm ⁻¹)	76.5 ± 9.1	56.7 ± 7.0	63.6 ± 4.2	32.7 ± 7.4*
BFR (μm ³ /μm ² /Year)	104.1 ± 12.1	66.9 ± 8.8	62.7 ± 7.3	40.4 ± 6.1**
OcS/BS	7.75 ± 0.3	7.91 ± 0.2	7.83 ± 0.5	7.52 ± 0.4

Figure S6

Histomorphometric analysis of vertebrae of WT, single (*Lrp5*+/-, *Runx2*+/-, *Osx*+/-, *Atf4*+/- or *Creb_{osb}*+/-) and double (*Lrp5*+/-;*Runx2*+/-, *Lrp5*+/-;*Osx*+/-, *Lrp5*+/-;*Atf4*+/- or *Lrp5*+/-;*Creb_{osb}*+/-) heterozygous mutant mice.

Figure S7. Genetic interaction between Lrp5 and serotonin

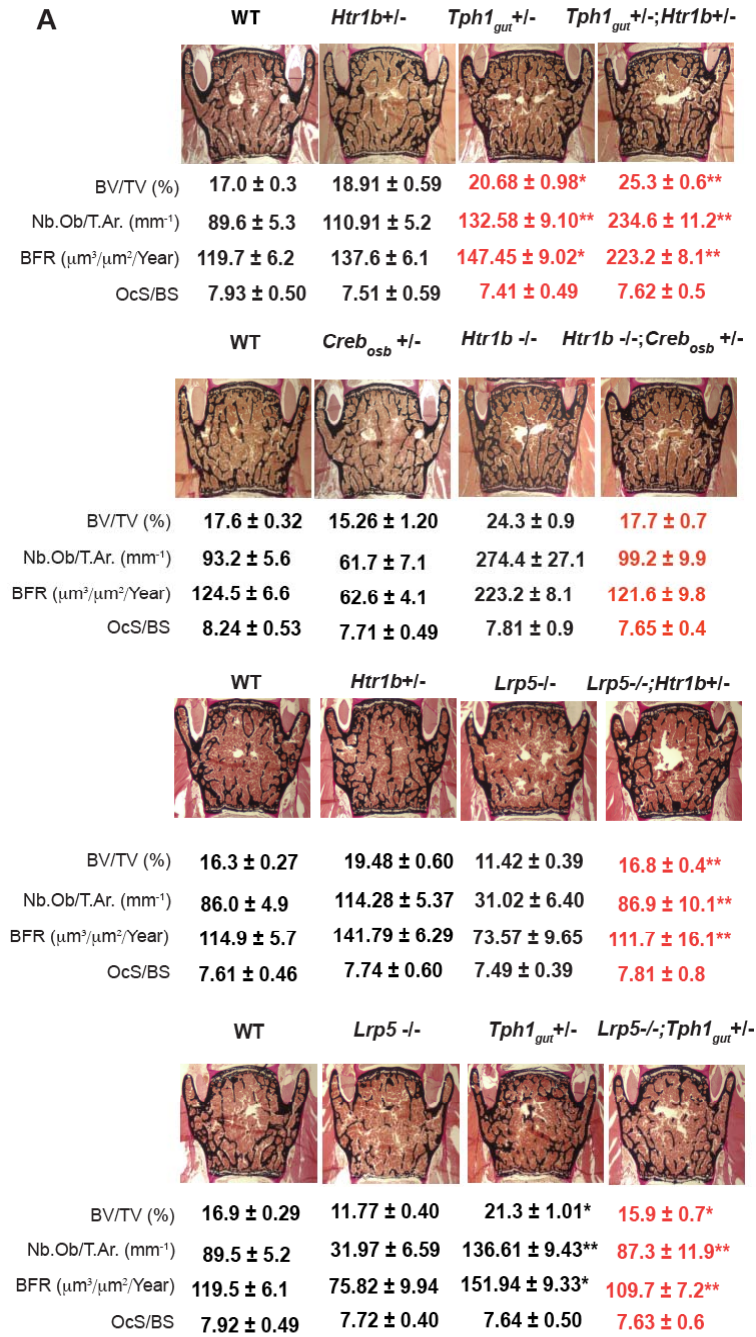


Figure S7.

(A) Bone histomorphometric analysis (vertebrae) of WT, *Htr1b*^{+/-}, *Tph1*_{gut}^{+/-}, *Htr1b*^{+/-};*Tph1*_{gut}^{+/-}, *Lrp5*^{-/-}, *Lrp5*^{-/-};*Htr1b*^{+/-} and *Lrp5*^{-/-};*Tph1*_{gut}^{+/-} mice.

Figure S7. Generation of mice lacking one allele of β -Catenin in the gut

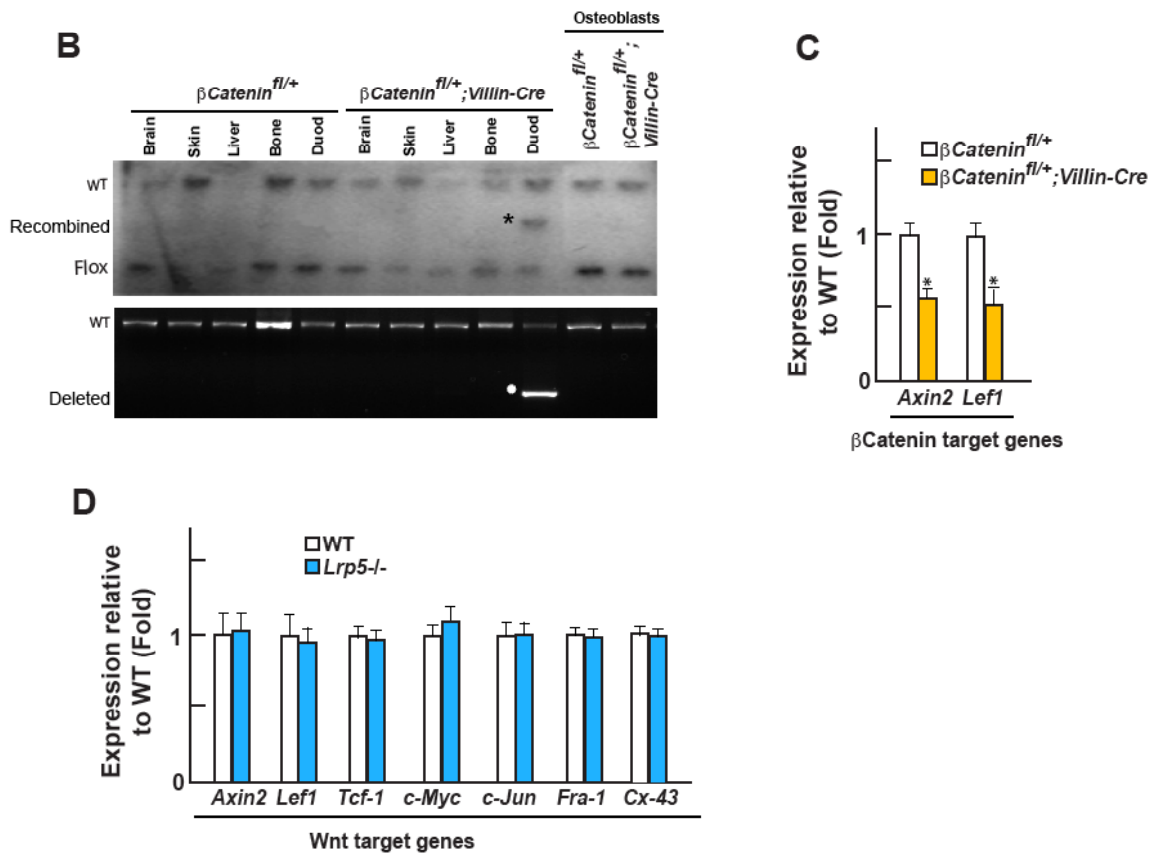


Figure S7

(B) Recombination analysis of β -Catenin locus in different tissues of β -Catenin^{fl/+} and β -Catenin^{fl/+};Villin-Cre mice using southern blotting and PCR on genomic DNA. Asterisks indicate the recombined or the deleted allele.

(C) Real-time PCR analysis of β -Catenin-target genes in the duodenum of WT and β -Catenin^{fl/+};Villin-Cre mice (n=3).

(D) Real-time PCR analysis of Wnt-target genes in the duodenum of WT and Lrp5^{-/-} mice (n>6).

Figure S8. Representative bone histomorphometric sections of mutant mouse strains

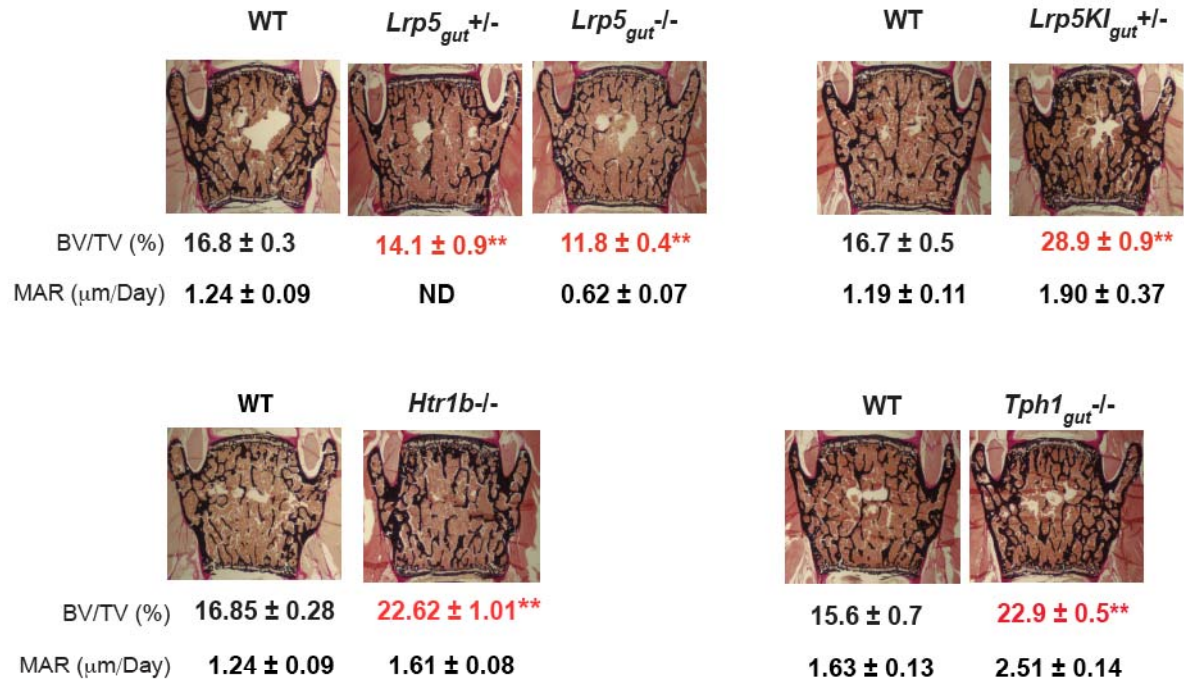


Figure S8.

Representative bone histomorphometric sections of WT, *Lrp5_{gut}^{+/-}*, *Lrp5_{gut}^{-/-}*, *Lrp5KI_{gut}^{+/-}*, *Htr1b^{-/-}* and *Tph1_{gut}^{-/-}* mice at 3 months of age (ND: not determined).

Figure S9. Gene expression profiling in the long bones of mutant mouse strains

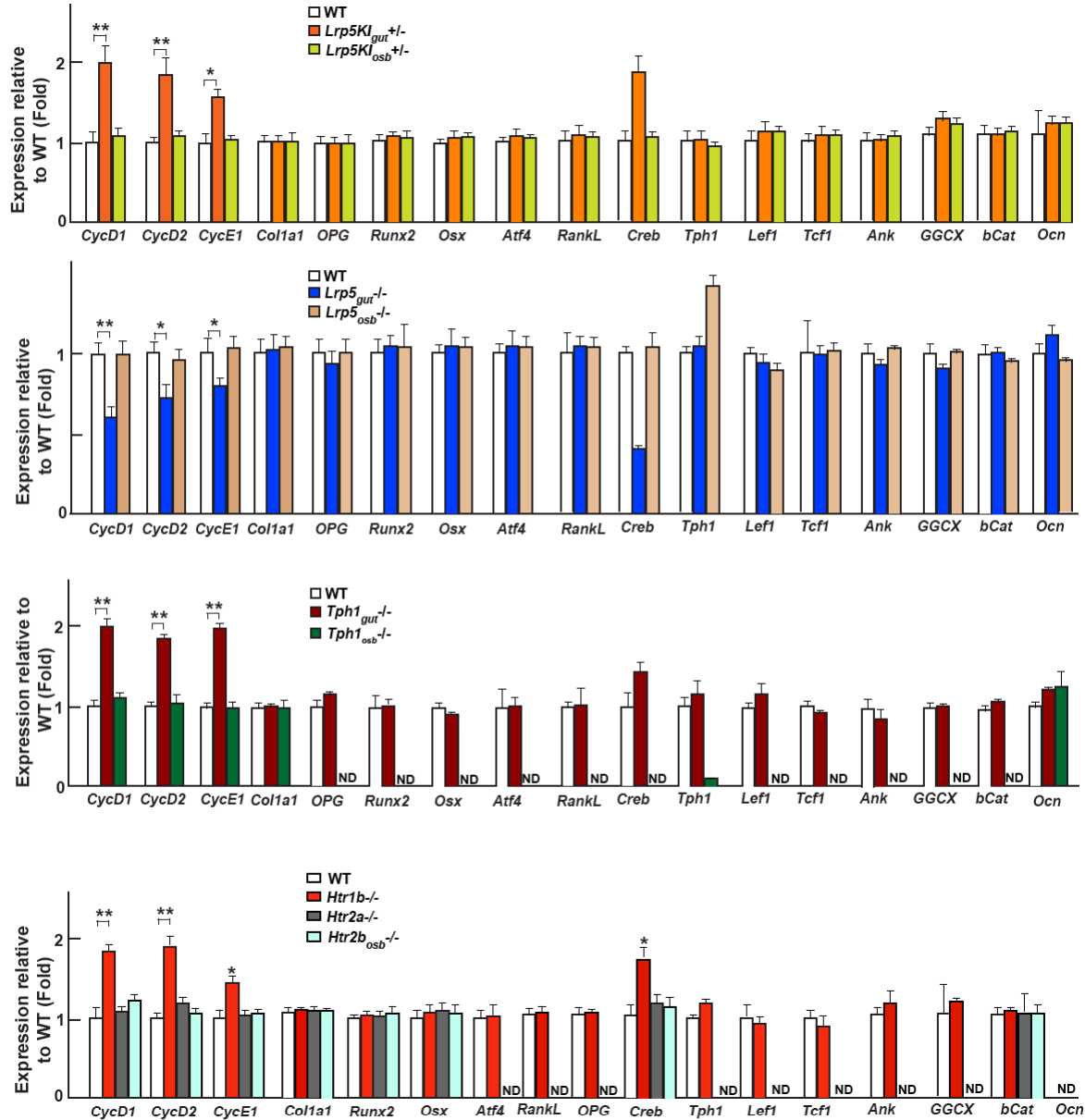


Figure S9.

Gene expression analysis in the bone collected from WT, *Lrp5^{gut}-/-*, *Lrp5^{osb}-/-*, *Lrp5^{KIgut}+/-*, *Lrp5^{KIosb}+/-*, *Tph1^{osb}-/-*, *Htr1b*-/-, *Htr2a*-/-, *Htr2b^{osb}-/-* and *Tph1^{gut}-/-* mice (ND: not determined).

Figure S10. Serum biochemistry of different mutant mice

Genotype	Ca (mg/dL)	Pi (mg/dL)	E (ng/mL/mmoles Creatinine)	NE (ng/mL/mmoles Creatinine)	PTH (ng/mL)	Leptin (ng/mL)
<i>Lrp5</i> ^{+/+}	9.21 ± 0.03	7.37 ± 0.02	22.14 ± 5.46	25.89 ± 6.03	0.112 ± 0.03	5.12 ± 0.72
<i>Lrp5</i> ^{-/-}	9.14 ± 0.02	7.71 ± 0.11	22.89 ± 3.28	25.51 ± 6.23	0.119 ± 0.01	4.10 ± 0.61
<i>Lrp5_{gut}</i> ^{+/+}	9.47 ± 0.03	7.57 ± 0.02	14.31 ± 1.69	34.57 ± 10.02	0.134 ± 0.02	5.97 ± 1.32
<i>Lrp5_{gut}</i> ^{-/-}	9.51 ± 0.08	7.89 ± 0.05	16.31 ± 1.58	33.50 ± 7.18	0.116 ± 0.05	4.71 ± 0.65
<i>Lrp5Kl_{gut}</i> ^{+/+}	9.28 ± 0.03	7.43 ± 0.02	21.18 ± 4.81	20.19 ± 2.52	ND	ND
<i>Lrp5Kl_{gut}</i> ^{+/-}	9.29 ± 0.02	7.27 ± 0.02	23.62 ± 0.70	25.53 ± 5.32	ND	ND
<i>Htr1b</i> ^{+/+}	8.98 ± 0.53	7.39 ± 0.02	13.53 ± 0.59	30.03 ± 8.73	0.095 ± 0.006	4.51 ± 0.82
<i>Htr1b</i> ^{-/-}	9.19 ± 0.22	7.53 ± 0.06	14.65 ± 0.98	29.27 ± 4.71	0.089 ± 0.007	5.53 ± 1.16

Figure S11. Histological analysis of gut in WT, *Lrp5*^{-/-}, *Lrp5*_{gut}^{-/-} and *Lrp5KI*_{gut}^{+/-} mice

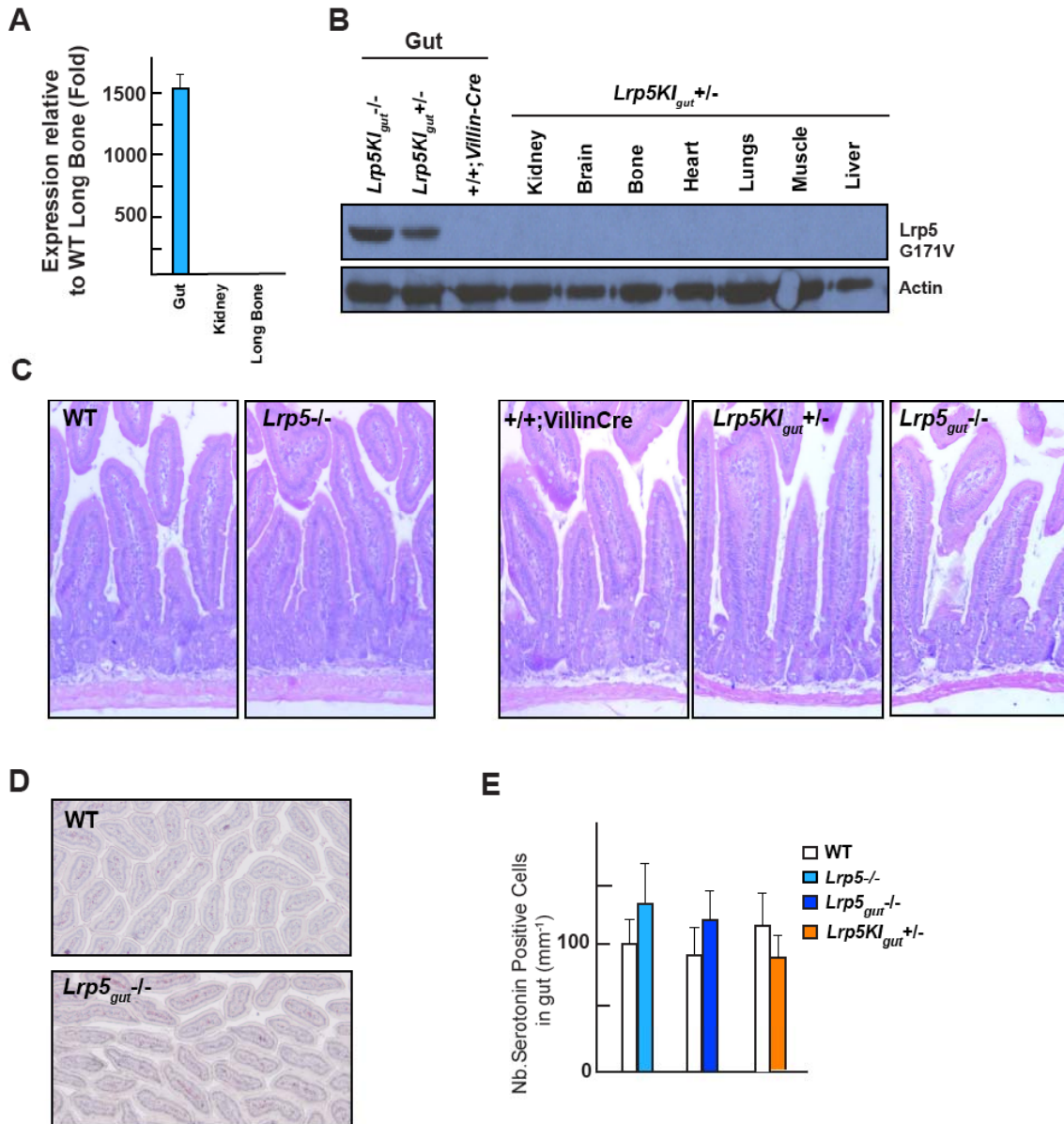


Figure S11.

(A) Relative *Tph1* expression in gut kidney and long bone.

(B) Expression of *Lrp5KI* in different tissues collected from WT, +/+;VillinCre and *Lrp5KI*_{gut}^{+/-} mice detected by Flag western blotting.

(C) Representative hematoxylin and eosin stained gut sections from WT, *Lrp5*^{-/-}, +/+;VillinCre, *Lrp5*_{gut}^{-/-} and *Lrp5KI*_{gut}^{+/-} mice.

(D) Representative serotonin immunostaining in the gut sections from WT and *Lrp5*_{gut}^{-/-} mice.

(E) Quantification of serotonin positive enterochromaffin cells in the gut of WT, *Lrp5*^{-/-}, +/+;VillinCre, *Lrp5*_{gut}^{-/-} and *Lrp5KI*_{gut}^{+/-} mice.